Progress In Electromagnetics Research C, Vol. 94, 233–245, 2019

A CPW-Fed Denim Based Wearable Antenna with Dual Band-Notched Characteristics for UWB Applications

Sulakshana Chilukuri* **and Shrinidhi Gogikar**

Abstract—This paper presents design analysis of a compact CPW-fed Wearable Textile Antenna with Dual Band notched characteristics for UWB applications. The proposed wearable textile antenna is designed on two different dielectric substrates; leather and denim with copper foil as conducting element. The performances of the designed textile antenna are compared on two substrates. Band-notched filtering characteristics are achieved by inserting semicircular split ring resonators on the conducting element. The first notch band is obtained from 2.3–2.5 GHz for Bluetooth application band, and the second notch band is obtained from 3.3–3.6 GHz for WiMAX application band. The simulated and measured frequency results show that the antenna has an impedance bandwidth of 1.8–10 GHz and reflection coefficient less than −10 dB, except at the two eliminating bands. The proposed antenna is designed and simulated using Ansys HFSS Electromagnetic Simulator. The prototype of the antenna has been developed on the denim substrate, and its performance is measured and compared with the simulated ones.

1. INTRODUCTION

From the past few years, the rapid progress in the development of wearable computing potentially increased the demand for body-worn devices which could be easily integrated with fabrics. Wearable textile antennas can be one of these devices. Generally, wearable antennas consist of a conducting material (patch/radiating element), printed on a dielectric substrate. The dielectric substrate can be any fabric/textile-like cordura, cotton, polycot, jeans cotton, denim, leather, fleece, etc. Flectron, Shieldit Super, Shieldex Nora, Zelt, Copper foil, and Pure copper taffeta fabric are the few commonly used conducting materials [1]. These antennas have gained much attention due to their robustness, small profile, flexibility, simple design, light weight, ease of integration into the garments, and its sustainable optimum performance [2, 3]. Because of these advantages, wearable textile antennas have a wide range of applications in the area of medical stream [3–5], public safety [6], emergency rescue systems [7], navigation [8], entertainment, aeronautics, tracking a person in defense and mining [9, 10] and have also found a solution for the implementation of wireless body area network (WBAN) [2, 11–13], on-off-body [14–17], and Body Centric wireless communications (BCWC) [18–20]. In open literature, several topologies have been presented for the development of the wearable textile antennas which include 3D printing technology [21, 22], PIFA [11, 23, 24], IIFA [25], Substrate Integrated Waveguide technology (SIW) [14, 16, 26, 27], aperture coupled [28, 29], microstrip patch [16, 17], CPW fed [2, 21, 30, 31], EGB based [4, 32, 33], meta material based [34, 35], and cavity based textile antennas [36, 37].

The introduction of unlicensed ultra-wideband (UWB) by the Federal Communications Commission (FCC) has attracted research interest in realizing UWB antennas for wireless applications. UWB technology allows implementation of multiple applications on a single antenna and also offers low-power

Received 21 May 2019, Accepted 23 July 2019, Scheduled 1 August 2019
* Corresponding author: Sulakshana Chilukuri (sulakshana@vardhaman.org).
The authors are with the Department of Electronics and Communication Engineering, Vardhaman College of Engineering, Hyderabad, India.

operation, extremely low radiated power, high capacity, multipath robustness, and multi-access, thus is very attractive for body-worn battery-operated devices [38]. Most of the UWB antennas obtain their wideband property by using wideband planar monopole concept as in [21], introducing slots on the radiating element/ground plane [39–41], tapered-shape slots [42–44], designing radiating element and a ground plane structure in the form of half circle [45], and partial ground plane structures [38, 46]. UWB antennas are suitable to cover mobile and wireless services and to reduce the system complexity by reduction of the overall device dimensions and costs. Therefore, merging UWB technology with wearable computing would be advantageous. But the primary issue with the UWB antennas is that their operation may interfere with other wireless communication systems. To minimize this interference problem, UWB antennas can be designed with notched-band characteristics. Various methods have been studied to achieve band rejection functionality in antennas such as etching out different shapes of slots [39, 45, 47], E-shape slot [48], half-wavelength and quarter-wavelength types of slots [49, 50], square slot [46] in the patch, H-shaped structure on the rear side of the antenna [51], using conventional methods of band notching like placing T-shaped parasitic strip in ground plane and a complimentary single split ring resonator (CSSR) on the patch [52], incorporating the electric ring resonator (ERR) [53], complementary split ring resonator (CSRR) with a CPW structure [54], placing S-shaped slits cut in the ground plane, an elliptical ring slot (ERS) in the patch [55], and placing dual mushroom-type electromagnetic-band gap (EBG) structures on the CPW feeding line [56].

In this paper, a wearable textile antenna with dual band-notched characteristics for UWB applications has been designed on leather as well as on denim, and results are compared. The notch frequencies in the passband of UWB are introduced by etching semicircular ring resonators in the patch. To the best of the authors' knowledge, very few wearable textile antennas have been designed for UWB applications, and no antenna has band notched characteristics. The proposed antenna is the only one with dual band notched characteristics that works for UWB application. Ansys HFSS Electromagnetic Simulator has been used for simulations, and results are presented. The geometrical configuration is presented in Section 2. The design approach and simulated results are discussed in Section 3. Antenna performance is described in Section 4. Finally, Section 5 presents the conclusion of the proposed antenna.

2. ANTENNA GEOMETRY AND DESIGN

The fundamental design of the proposed antenna is shown in Figure 1. This antenna, namely Antenna 1, consists of a semicircular radiator with radius $R_1 = 20\,\text{mm}$ along with two semicircular split ring resonators (SSRR), mounted on a 2 mm thick leather substrate with a relative permittivity of 2.27 and loss tangent of 0.02, and is fed using coplanar waveguide transmission line with a gap, $g = 0.5\,\text{mm}$.

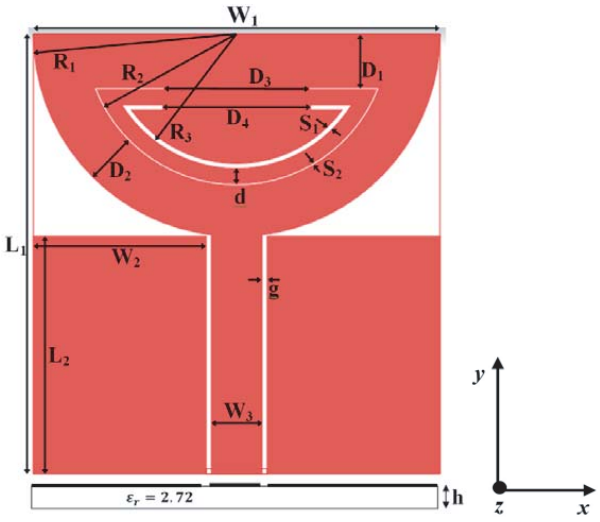

Figure 1. Geometrical structure of Antenna-1.

The conducting material used is copper foil. The overall dimensions of the proposed antenna are $43 \times 40 \times 2\,\text{mm}^3$. The radius of the semicircle is the analytical parameter to obtain a UWB frequency operation.

The final design of Antenna 1 is optimized taking several aspects into consideration such as bandwidth of the antenna, bandwidth of notched bands, and level of notched-bands. The optimized parameters used in this design are listed as follows: $L_1 = 43\,\text{mm}$, $W_1 = 40\,\text{mm}$, $L_2 = 23\,\text{mm}$, $W_2 = 17\,\text{mm}$, $W_3 = 5\,\text{mm}$, $R_1 = 20\,\text{mm}$, $R_2 = 13\,\text{mm}$, $R_3 = 12.5\,\text{mm}$, $g = 0.5\,\text{mm}$, $d = 1.5\,\text{mm}$, $D_1 = 5.3\,\text{mm}$, $D_2 = 5\,\text{mm}$, $D_3 = 14.2\,\text{mm}$, $D_4 = 14.5\,\text{mm}$, $S_1 = 0.2\,\text{mm}$, $S_2 = 0.5\,\text{mm}$, $h = 2\,\text{mm}$. Figure 2 demonstrates the evolution of the proposed antenna.

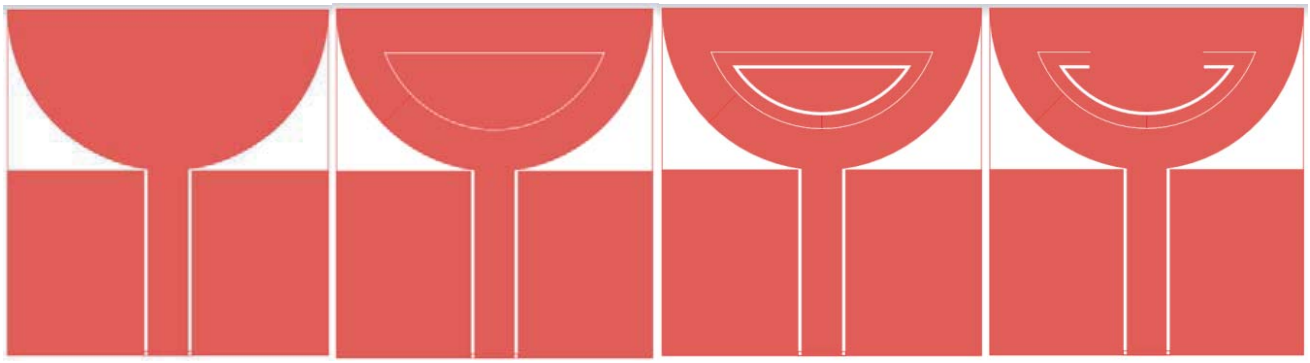

Figure 2. Evolution of the Antenna-1. (a) Ant 1, (b) Ant 2, (c) Ant 3, (d) Ant 4.

Figure 2(a) shows the basic antenna design. From this unique design, the antenna operates in the UWB frequency range, covering an impedance bandwidth ranging from 2.24 to 11.20 GHz. In order to achieve band-notched characteristics, Antenna 1 is modified by inserting a semi-circular ring slot into the radiating patch as shown in Figure 2(b). As a result of this modified structure, a single notch is obtained. Another slot is added in the patch to achieve the second notch as shown in Figure 2(c). The closed ring structure of the slots has been modified as an open ring slot structure by splitting it from its center to tune the notch frequency to the desired frequency band by varying the distance between the two ends of the rings. Figure 2(d) represents the optimized design of Antenna-1 with two split ring resonator structure.

3. DESIGN APPROACH AND SIMULATED RESULTS

Antenna-1 had undergone several evolutions to achieve the desired performance. Parameters S_1, S_2, d, D_1, and D_2 were varied with a range of values as part of the optimization process. A semi-circular slot is embedded into the patch as shown in Figure 2(b) which is responsible for the introduction first notch. The width (S_1) of the slot is varied from 0.6 mm to 0.2 mm. Table 1 displays the notch band operation for different values of S_1, and the corresponding plot of return loss characteristics are shown in Figure 3.

From the data provided in Table 1, it is observed that as S_1 decreases the notch band shifts towards lower frequency, and the effective bandwidth of the notch slightly gets narrow. Therefore, the optimized value of S_1 is selected to be 0.2 mm. For the second notch at the higher frequency, another semi-circular ring slot, with width S_2, is inserted into the patch as shown in Figure 2(c). Simulations are performed for the combination of different values of S_1 and S_2 by optimizing the distance d between the two slots. The considerable distance between the two slots is optimized by varying d from 2.5 mm to 1 mm. In the first case, d is fixed as 1.5 mm, and the results are tabulated in Table 2. The return loss characteristics for data corresponding to Table 2 are displayed in Figure 4.

As mentioned previously and with observations made from the above return loss characteristics plot, the decrease in the slot width results in a shift of the first notch towards lower frequency and

Table 1. Parametric variation of slot width S_1.

Slot Width S_1 (mm)	Overall UWB (GHz)	Notch-band frequency range (GHz)	Notch Bandwidth (GHz)
0.6	2.01–9.03	3.43–4.37	0.94
0.5	2.06–8.54	3.38–4.26	0.88
0.3	2.03–10.80	3.28–4.04	0.76
0.2	2.07–11.01	3.01–3.59	0.58

Table 2. Parametric variations of slot widths S_1 and S_2.

Slot Width S_1 (mm)	Slot Width S_2 (mm)	Overall UWB (GHz)	1st Notch Frequency (GHz)	2nd Notch Frequency (GHz)
0.2	0.2	2.01–9.33	3.40–3.87	4.38–4.87
0.5	0.5	1.95–9.03	3.39–4.04	4.78–4.99
0.2	0.5	2.01–10.8	3.39–3.87	4.45–4.98

narrowing of the bandwidth of the notch frequency. Therefore, the optimized value of S_1 is selected to be 0.2 mm. From the simulations performed for the above three combinations, it is found that UWB is obtained for the third combination of 0.2 mm and 0.5 mm as slot widths for the first and second slots, respectively. The first slot with S_1 as 0.2 is responsible for the first notch whose bandwidth falls under IEEE 802.16 WiMAX application band (3.3–3.6 GHz covering 3.3 GHz and 3.5 GHz, respectively), and the second slot with S_2 as 0.5 mm is responsible for the second notch with the bandwidth applicable for rejecting AMT-fixed services application band (covering 4.5 GHz). Therefore, choosing the optimized values for S_1 and S_2 as 0.2 mm and 0.5 mm, respectively, the distance d between the two ring resonators is varied to observe further variations in the frequency shift of notched-bands. Here, d is set as 1 mm first and then increased by 2 mm. Table 3 displays the variation in frequency band shift as d varies from 1 mm to 2 mm, and also the return loss characteristics are plotted as shown in Figure 5.

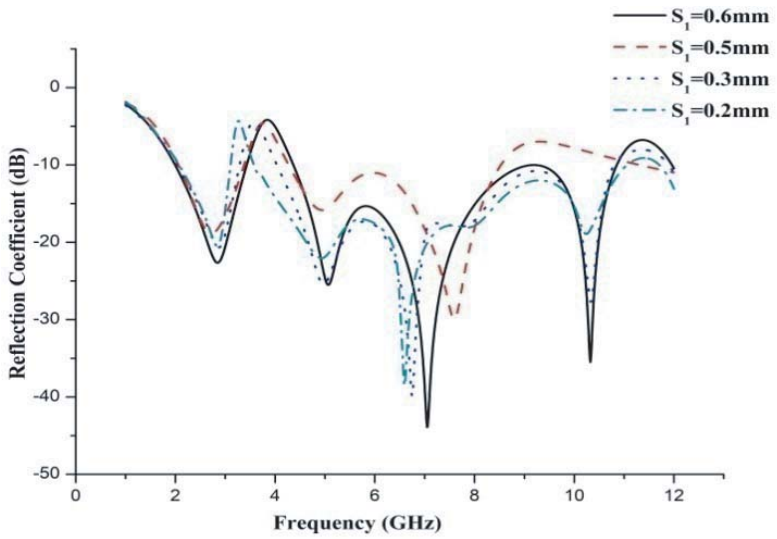

Figure 3. Comparison of notch band between the antennas with varying S_1.

Table 3. Parametric variations of the distances between the two slots.

Distance d (mm)	**$d = 1$ mm**	**$d = 2$ mm**
Overall UWB (GHz)	1.96–10.68	2.20–10.79
Notch 1 (GHz)	3.28–3.61	3.18–3.31
Notch 2 (GHz)	4.00–4.77	3.50–3.76
Notch 3 (GHz)	8.74–9.28	4.85–5.18
Notch 4 (GHz)	-	8.90–9.45

As we decrease d from 1.5 mm to 1 mm, the first two notches are under application bands, but there is an introduction of the third notch band which is inapplicable for rejecting any applications. When d is increased to 2 mm, four notch bands are introduced which are not following under any application rejection band. From the simulations carried out by varying the parameters like S_1, S_2, and d, the

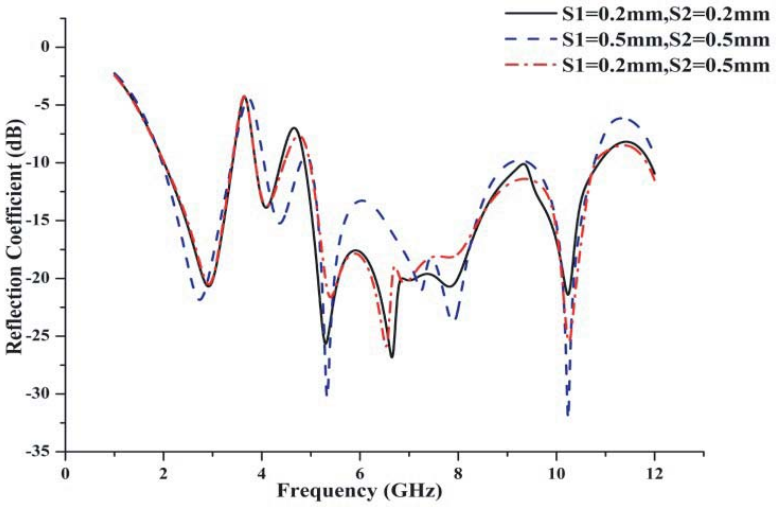

Figure 4. Comparison of notch-bands with varying slots S_1 and S_2.

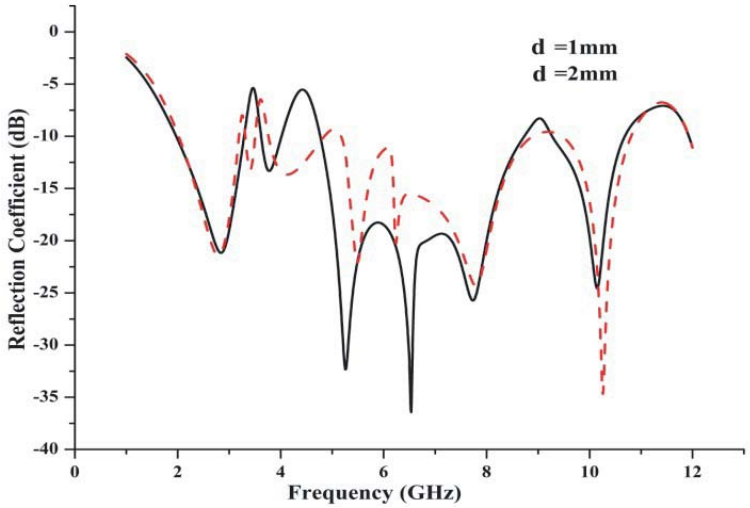

Figure 5. Comparison of notch bands by varying the distance d.

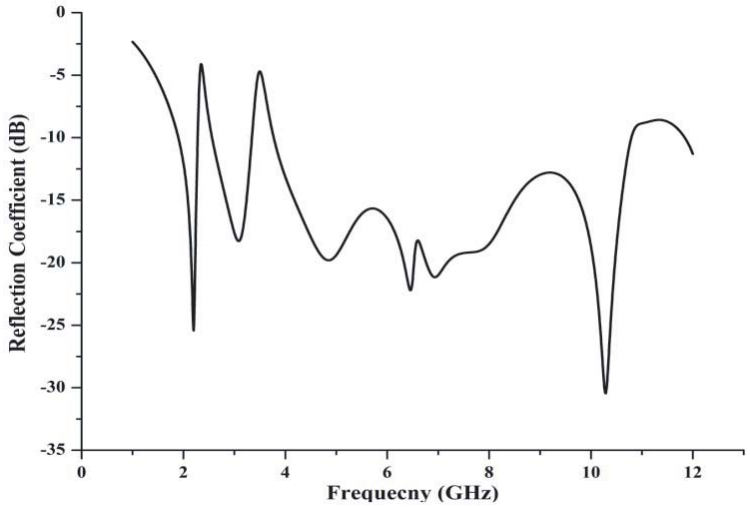

Figure 6. Reflection coefficient of the optimized design of Antenna-1.

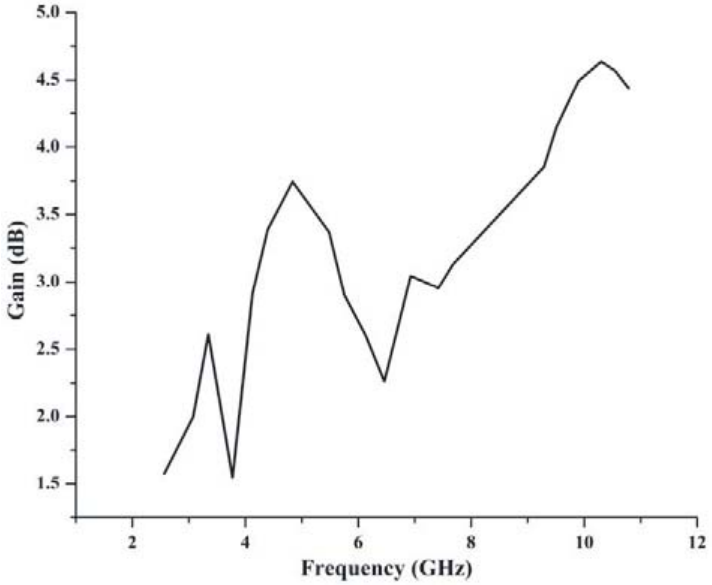

Figure 7. Simulated gain vs frequency plot for Antenna-1.

results obtained are not satisfactory to achieve the rejection of Bluetooth notch. To get the rejection property at 2.4 GHz and 3.3 to 3.6 GHz, the notch frequencies are shifted towards left by modifying the structure of closed ring slots to open ring slots. The ring's structure has been changed by splitting it from its center as shown in Figure 2(d). The distances $D_3 = 14.2$ mm and $D_4 = 14.5$ mm between the two ends of SSRS are varied to tune the frequency notched-band to fall under rejection band for desired applications. The return loss characteristics, for the optimized design of Antenna-1, are shown in Figure 6.

Figure 6 shows that the antenna operates with an impedance bandwidth of 1.8–10.7 GHz that includes UWB frequency and reflection coefficient less than -10 dB, except the two eliminated bands to reject the Bluetooth application band at 2.4 GHz and the WiMAX application band 3.3–3.6 GHz. Figure 7 shows the overall gain ranging from 1.5 to 4 dB for a frequency range of 1.8 to 10.7 GHz.

Taking the dimensions of Antenna-1, Antenna-2 has been designed on a 0.7 mm thick denim whose dielectric constant is 1.7 with a loss tangent of 0.05. The return loss characteristics of Antenna-2 are

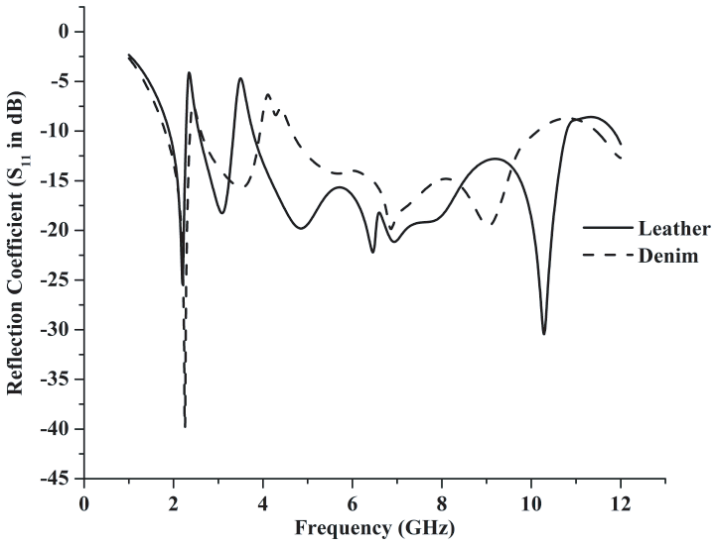

Figure 8. Comparison between the return loss characteristics of Antenna-1 and Antenna-2.

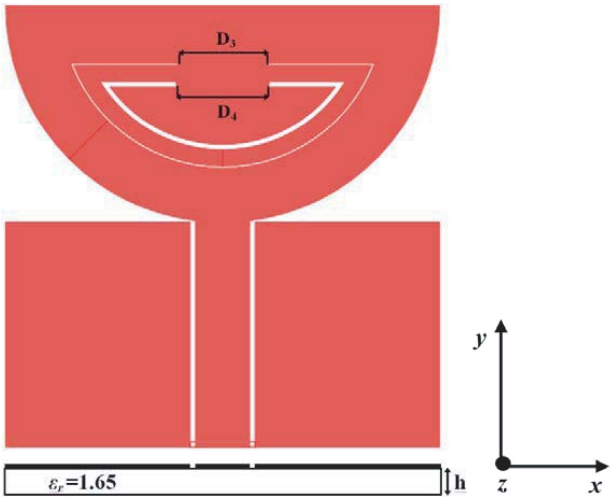

Figure 9. Modified dimensions of Antenna-2.

Figure 10. Fabricated prototype of Antenna-2.

compared with Antenna-1. The first notch for Antenna-2 is obtained from 2.3 to 2.6 GHz, but the second notch is achieved from 3.9 to 4.6 GHz which does not come under the WiMAX band. Figure 8 represents the comparison of the return loss characteristics between Antenna-1 and Antenna-2.

To make the band notches fall under Bluetooth and WiMAX application regions, Antenna-2 is further optimized by decreasing the distances D_1 and D_2 between the two ends of the split ring resonators. The modified structure of Antenna-2 with dimensions $D_1 = 8.2\,\text{mm}$, $D_2 = 8.5\,\text{mm}$, $h = 0.7\,\text{mm}$ is shown in Figure 9.

Finally, Antenna-2 is fabricated on denim with these modified dimensions, and the fabricated prototype is displayed in Figure 10.

4. ANTENNA PERFORMANCE

Measured and simulated return loss characteristics of Antenna-2 are shown in Figure 11. Simulated results cover impedance bandwidth less than $-10\,\text{dB}$ ranging from 1.8 to 10 GHz that includes the UWB

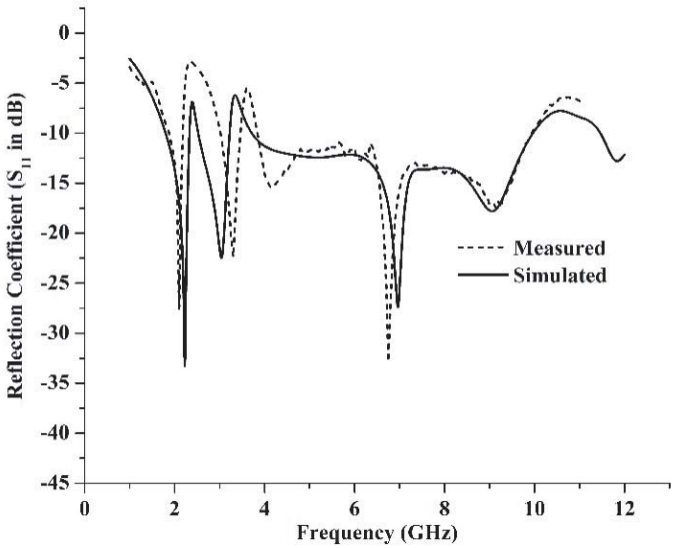

Figure 11. Measured and simulated return loss characteristics.

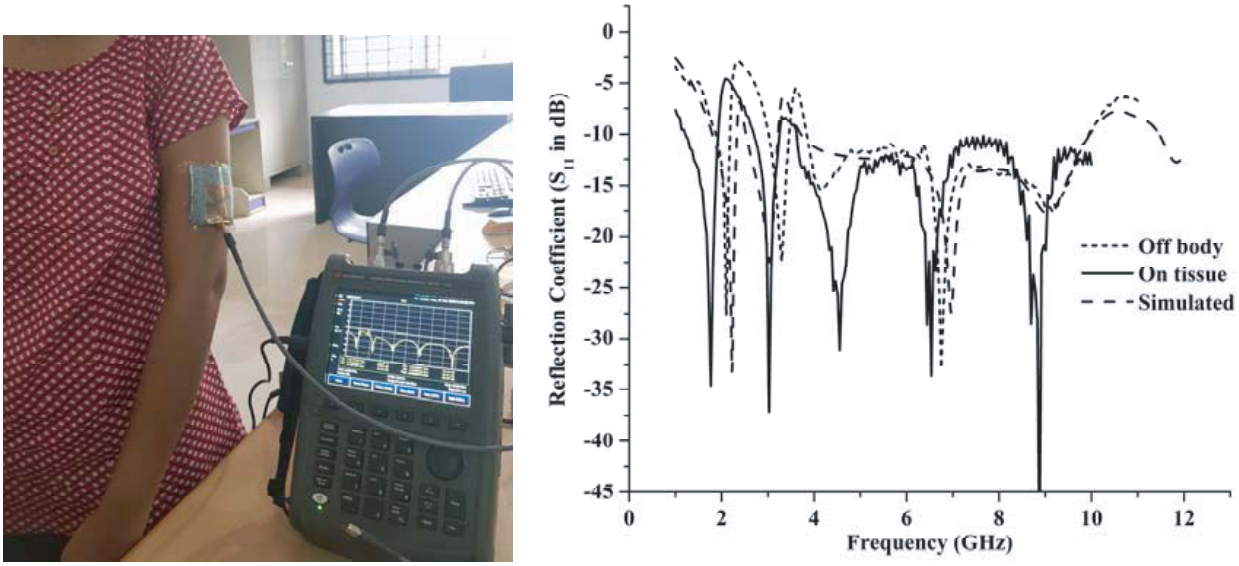

Figure 12. (a) On-body measurement setup and (b) simulated and measured (off-body and on-body) return loss characteristics of Antenna-2.

frequency range with dual notch bands, one from 2.3 to 2.5 GHz and the other from 3.2 to 3.7 GHz. The measured results slightly vary from simulated ones due to fabrication inaccuracy.

To study the on-body performance, the antenna is placed on the tissue of female human volunteer. The on-body S_{11} performance is evaluated by placing the antenna on arm of the human body as shown in the photograph in Figure 12(a). The reflection coefficient (S_{11}) is measured in the frequency range 1 to 10 GHz using a Keysight Foxfield Microwave Analyzer N9916A that works up to 14 GHz in Network Analyzer mode.

Figure 12(b) indicates the comparison between simulated and measured (Off-body and On-body) S_{11} characteristics of Antenna-2. It is observed from the on-body measured results that two notch bands are shifted towards lower band of frequencies compared with off-body measurements. The two notch bands are 2 to 2.6 GHz and 3.3 to 3.6 GHz, respectively.

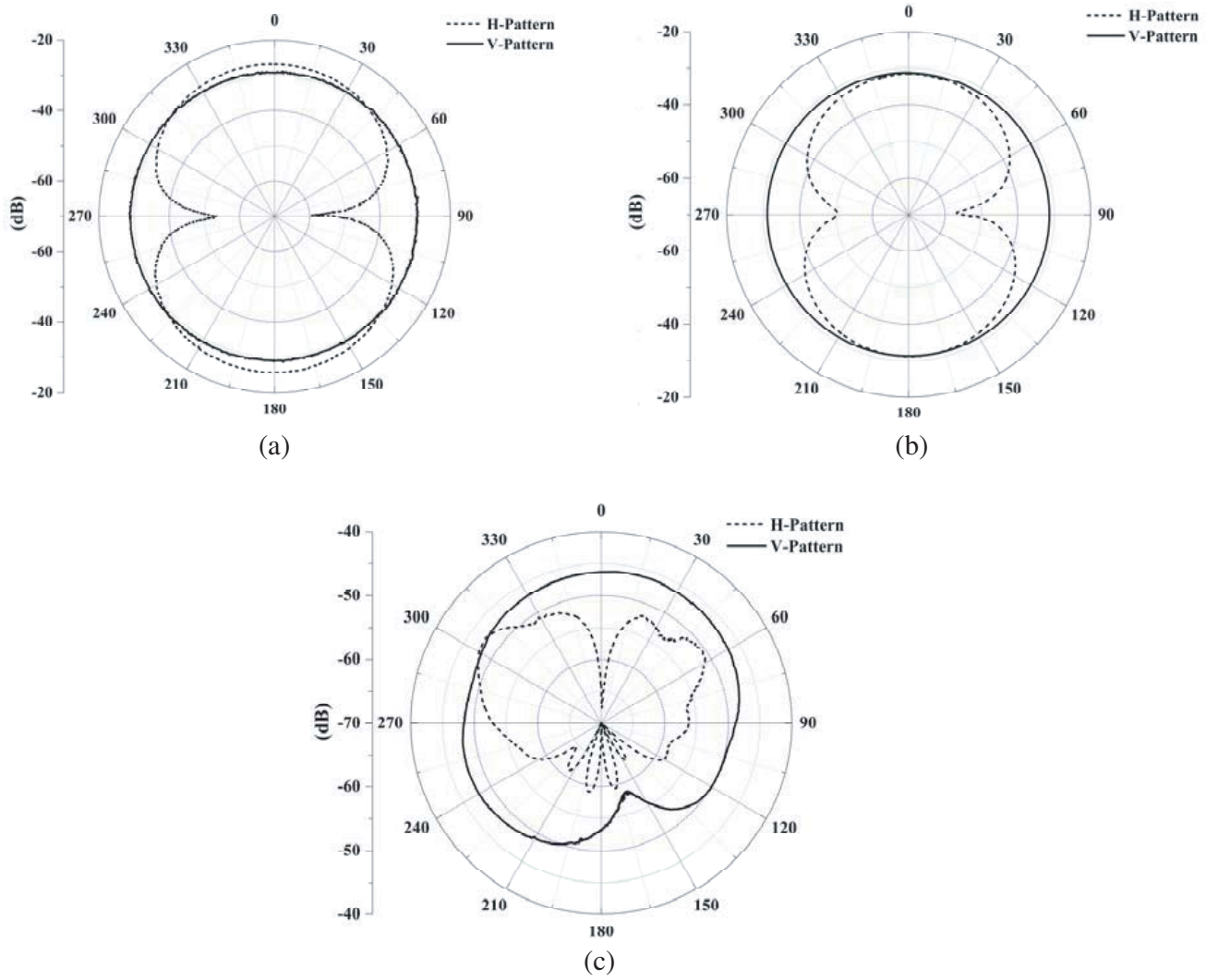

Figure 13. (a) Radiation pattern at 2.09 GHz. (b) Radiation pattern at 3.28 GHz. (c) Radiation pattern at 6.47 GHz.

Table 4. Comparison of Antenna-2 with other UWB textile antenna.

Ref no.	Conducting Material	Substrate	UWB Range (GHz)	Max Gain (dB)	No. of notch bands
This Work	Copper	Denim	1.8–10	5.09	2
[2]	Nora	Acrylic	3.1–10.6	Not Evaluated	-
[17]	ShieldIt Super	Felt	3–10	7.75	-
[19]	Copper	Cotton	3.1–10.6	Not Evaluated	-
[30]	ShieldIt	Felt	3.1–10.6	Not Evaluated	-
[31]	ShieldIt	Denim Jeans	2–12	Not Evaluated	-

Radiation patterns are evaluated at three different frequencies 2.09, 3.28, and 6.74 GHz in both horizontal (xy-plane) and vertical planes (yz-planes).

A figure of 8 pattern is obtained in horizontal plane and omnidirectional pattern in vertical plane

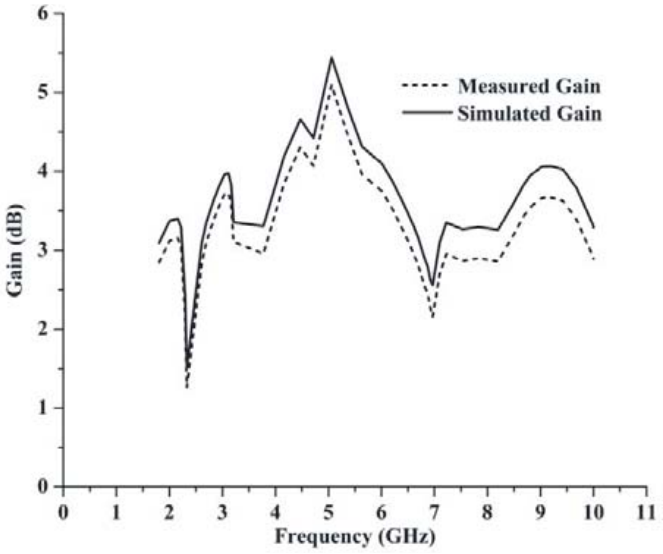

Figure 14. Measured and simulated gain vs frequency plot.

at 2.09 and 3.28 GHz as shown in Figure 13(a) and Figure 13(b), respectively. Directional radiation pattern is observed at 6.74 GHz shown in Figure 13(c).

Figure 14 depicts the measured and simulated gains of Antenna-2. The measured result shows that overall gain varies from 1.26 to 5.09 dB for the UWB range covering from 1.8 to 10 GHz.

Table 4 presents the comparison of several wearable UWB antennas available in the literature. It is observed from the table that the proposed antenna works for UWB applications with two notch bands with moderate gain where the other antennas have no notch band characteristics. This is the major advantage of the proposed antenna.

5. CONCLUSION

A CPW-fed Wearable Textile Antenna with Dual Band-notched characteristics for UWB applications is designed on both leather and denim dielectric textile materials and simulated using Ansys HFSS Electromagnetic Simulator. The measured results of denim antenna are compared with simulated results. The property of dual band notched characteristics is achieved by employing split ring resonators into the semi-circular patch of the antenna. The simulated results show that the realized dual band-notched antenna has an impedance bandwidth from 1.8 to 10 GHz and reflection coefficient less than −10 dB with dual notched bands centered at 2.4 GHz (Bluetooth application band) and 3.3–3.6 GHz (WiMAX IEEE 802.16 application band). Stable radiation patterns are obtained for the UWB for the gain over a range of 1.26–5.5 dB. The antenna is compact and simple in structure. The proposed antenna can be used for wearable UWB body worn Bluetooth, WiMAX interference free application.

REFERENCES

1. Cicchetti, R., E. Miozzi, and O. Testa, "Wideband and UWB antennas for wireless applications: A comprehensive review," *International Journal of Antennas and Propagation*, Vol. 2017, 1–45, 2017.
2. Yimdjo Poffelie, L. A., P. J. Soh, S. Yan, and G. A. E. Vandenbosch, "A high-fidelity all-textile UWB antenna with low back radiation for off-body WBAN applications," *IEEE Transactions on Antennas and Propagation*, Vol. 64, No. 2, 757–760, Feb. 2016.
3. Ashyap, A. Y. I., et al., "Inverted E-shaped wearable textile antenna for medical applications," *IEEE Access*, Vol. 6, 35214–35222, 2018.
4. Ashyap, A. Y. I., et al., "Compact and low-profile textile EBG-based antenna for wearable medical applications," *IEEE Antennas and Wireless Propagation Letters*, Vol. 16, 2550–2553, 2017.

5. Soh, P. J., et al., "A smart wearable textile array system for biomedical telemetry applications," *IEEE Transactions on Microwave Theory and Techniques*, Vol. 61, No. 5, 2253–2261, May 2013.
6. Crespo-Bardera, M. Sanchez-Fernandez, A. Garcia-Armada, A. G. Martin, and A. F. Duran, "Analysis of a LTE-based textile massive MIMO proposal for public safety networks," *IEEE 86th Vehicular Technology Conference (VTC-Fall)*, 1–5, Toronto, ON, 2017.
7. Hussin, E. F. N. M., et al., "A wearable textile dipole for search and rescue application," *5th International Conference on Electronic Devices, Systems and Applications (ICEDSA)*, 1–4, Ras Al Khaimah, 2016.
8. Kaivanto, E. K., M. Berg, E. Salonen, and P. de Maagt, "Wearable circularly polarized antenna for personal satellite communication and navigation," *IEEE Transactions on Antennas and Propagation*, Vol. 59, No. 12, 4490–4496, Dec. 2011.
9. Lee, H., J. Tak, and J. Choi, "Wearable antenna integrated into military berets for indoor/outdoor positioning system," *IEEE Antennas and Wireless Propagation Letters*, Vol. 16, 1919–1922, 2017.
10. Hertleer, C., H. Rogier, L. Vallozzi, and L. van Langenhove, "A textile antenna for off-body communication integrated into protective clothing for firefighters," *IEEE Transactions on Antennas and Propagation*, Vol. 57, No. 4, 919–925, Apr. 2009.
11. Gao, G., C. Yang, B. Hu, R. Zhang, and S. Wang, "A wearable PIFA with an all-textile metasurface for 5 GHz WBAN applications," *IEEE Antennas and Wireless Propagation Letters*, Vol. 18, No. 2, 288–292, Feb. 2019.
12. Hong, Y., J. Tak, and J. Choi, "An all-textile SIW cavity-backed circular ring-slot antenna for WBAN applications," *IEEE Antennas and Wireless Propagation Letters*, Vol. 15, 1995–1999, 2016.
13. Yan, S., P. J. Soh, and G. A. E. Vandenbosch, "Wearable dual-band magneto-electric dipole antenna for WBAN/WLAN applications," *IEEE Transactions on Antennas and Propagation*, Vol. 63, No. 9, 4165–4169, Sep. 2015.
14. Lajevardi, M. E. and M. Kamyab, "Ultraminiaturized metamaterial-inspired SIW textile antenna for off-body applications," *IEEE Antennas and Wireless Propagation Letters*, Vol. 16, 3155–3158, 2017.
15. Xiaomu, H., S. Yan, and G. A. E. Vandenbosch, "Wearable Button Antenna For Dual-Band WLAN applications with combined on and off-body radiation patterns," *IEEE Transactions on Antennas and Propagation*, Vol. 65, No. 3, 1384–1387, Mar. 2017.
16. Mendes, C. and C. Peixeiro, "On-body transmission performance of a novel dual-mode wearable microstrip antenna," *IEEE Transactions on Antennas and Propagation*, Vol. 66, No. 9, 4872–4877, Sep. 2018.
17. Samal, P. B., P. J. Soh, and G. A. E. Vandenbosch, "UWB all-textile antenna with full ground plane for off-body WBAN communications," *IEEE Transactions on Antennas and Propagation*, Vol. 62, No. 1, 102–108, Jan. 2014.
18. Simorangkir, R. B. V. B., Y. Yang, L. Matekovits, and K. P. Esselle, "Dual-band dual-mode textile antenna on PDMS substrate for body-centric communications," *IEEE Antennas and Wireless Propagation Letters*, Vol. 16, 677–680, 2017.
19. Sun, Y., S. W. Cheung, and T. I. Yuk, "Design of a textile ultra-wideband antenna with stable performance for body-centric wireless communications," *IET Microwaves, Antennas & Propagation*, Vol. 8, No. 15, 1363–1375, Sep. 12, 2014.
20. Koski, K., L. Sydänheimo, Y. Rahmat-Samii, and L. Ukkonen, "Fundamental characteristics of electro-textiles in wearable UHF RFID patch antennas for body-centric sensing systems," *IEEE Transactions on Antennas and Propagation*, Vol. 62, No. 12, 6454–6462, Dec. 2014.
21. Jun, S., B. Sanz-Izquierdo, and M. Summerfield, "UWB antenna on 3D printed flexible substrate and foot phantom," *Loughborough Antennas & Propagation Conference (LAPC)*, 1–5, Loughborough, 2015.
22. Cosker, M., L. Lizzi, F. Ferrero, R. Staraj, and J. Ribero, "Realization of 3-D flexible antennas using liquid metal and additive printing technologies," *IEEE Antennas and Wireless Propagation Letters*, Vol. 16, 971–974, 2017.

23. Yan, S., V. Volskiy, and G. A. E. Vandenbosch, "Compact dual-band textile PIFA for 433-MHz/2.4-GHz ISM bands," *IEEE Antennas and Wireless Propagation Letters*, Vol. 16, 2436–2439, 2017.
24. Ivsic, B., D. Bonefacic, and J. Bartolic, "Considerations on embroidered textile antennas for wearable applications," *IEEE Antennas and Wireless Propagation Letters*, Vol. 12, 1708–1711, 2013.
25. El Hajj, W., C. Person, and J. Wiart, "A novel investigation of a broadband integrated inverted-F antenna design; Application for wearable antenna," *IEEE Transactions on Antennas and Propagation*, Vol. 62, No. 7, 3843–3846, Jul. 2014.
26. Moro, R., S. Agneessens, H. Rogier, and M. Bozzi, "Circularly-polarised cavity-backed wearable antenna in SIW technology," *IET Microwaves, Antennas & Propagation*, Vol. 12, No. 1, 127–131, Oct. 1, 2018.
27. Agneessens, S., "Coupled eighth-mode substrate integrated waveguide antenna: Small and wideband with high-body antenna isolation," *IEEE Access*, Vol. 6, 1595–1602, 2018.
28. Zhang, J., S. Yan, and G. A. E. Vandenbosch, "A miniature feeding network for aperture-coupled wearable antennas," *IEEE Transactions on Antennas and Propagation*, Vol. 65, No. 5, 2650–2654, May 2017.
29. Hertleer, C., A. Tronquo, H. Rogier, L. Vallozzi, and L. van Langenhove, "Aperture-coupled patch antenna for integration into wearable textile systems," *IEEE Antennas and Wireless Propagation Letters*, Vol. 6, 392–395, 2007.
30. Klemm, M. and G. Troester, "Textile UWB antennas for wireless body area networks," *IEEE Transactions on Antennas and Propagation*, Vol. 54, No. 11, 3192–3197, Nov. 2006.
31. Yahya, R., M. R. Kamarudin, and N. Seman, "Effect of rainwater and seawater on the permittivity of denim jean substrate and performance of UWB eye-shaped antenna," *IEEE Antennas and Wireless Propagation Letters*, Vol. 13, 806–809, 2014.
32. Lin, X., B. Seet, F. Joseph, and E. Li, "Flexible fractal electromagnetic bandgap for millimeter-wave wearable antennas," *IEEE Antennas and Wireless Propagation Letters*, Vol. 17, No. 7, 1281–1285, Jul. 2018.
33. Zhu, S. and R. Langley, "Dual-band wearable textile antenna on an EBG substrate," *IEEE Transactions on Antennas and Propagation*, Vol. 57, No. 4, 926–935, Apr. 2009.
34. Tak, J. and J. Choi, "A wearable metamaterial microwave absorber," *IEEE Antennas and Wireless Propagation Letters*, Vol. 16, 784–787, 2017.
35. Yan, S., P. J. Soh, and G. A. E. Vandenbosch, "Compact all-textile dual-band antenna loaded with metamaterial-inspired structure," *IEEE Antennas and Wireless Propagation Letters*, Vol. 14, 1486–1489, 2015.
36. Pinapati, S. P., D. C. Ranasinghe, and C. Fumeaux, "Textile multilayer cavity slot monopole for UHF applications," *IEEE Antennas and Wireless Propagation Letters*, Vol. 16, 2542–2545, 2017.
37. Liu, F., T. Kaufmann, Z. Xu, and C. Fumeaux, "Wearable applications of quarter-wave patch and half-mode cavity antennas," *IEEE Antennas and Wireless Propagation Letters*, Vol. 14, 1478–1481, 2015.
38. Klemm, M. and G. Troester, "Textile UWB antennas for wireless body area networks," *IEEE Transactions on Antennas and Propagation*, Vol. 54, No. 11, 3192–3197, Nov. 2006.
39. Ren, J., W. Hu, Y. Yin, and R. Fan, "Compact printed MIMO antenna for UWB applications," *IEEE Antennas and Wireless Propagation Letters*, Vol. 13, 1517–1520, 2014.
40. Guo, Z., H. Tian, X. Wang, Q. Luo, and Y. Ji, "Bandwidth enhancement of monopole UWB antenna with new slots and EBG structures," *IEEE Antennas and Wireless Propagation Letters,* Vol. 12, 1550–1553, 2013.
41. Liu, W., Y. Yin, W. Xu, and S. Zuo, "Compact open-slot antenna with bandwidth enhancement," *IEEE Antennas and Wireless Propagation Letters*, Vol. 10, 850–853, 2011.
42. Azim, R., M. T. Islam, and N. Misran, "Compact tapered-shape slot antenna for UWB applications," *IEEE Antennas and Wireless Propagation Letters*, Vol. 10, 1190–1193, 2011.

43. Medeiros, C. R., J. R. Costa, and C. A. Fernandes, "Compact tapered slot UWB antenna with WLAN band rejection," *IEEE Antennas and Wireless Propagation Letters*, Vol. 8, 661–664, 2009.
44. Fortino, N., J. Dauvignac, G. Kossiavas, and R. Staraj, "Design optimization of UWB printed antenna for omnidirectional pulse radiation," *IEEE Transactions on Antennas and Propagation*, Vol. 56, No. 7, 1875–1881, Jul. 2008.
45. Bialkowski, M. E. and A. M. Abbosh, "Design of UWB planar antenna with improved cut-off at the out-of-band frequencies," *IEEE Antennas and Wireless Propagation Letters*, Vol. 7, 408–410, 2008.
46. Jangid, S. and M. Kumar, "A novel UWB band notched rectangular patch antenna with square slot," *Fourth International Conference on Computational Intelligence and Communication Networks, Mathura*, 5–9, 2012.
47. Jang, J. and H. Hwang, "An improved band-rejection UWB antenna with resonant patches and a slot," *IEEE Antennas and Wireless Propagation Letters*, Vol. 8, 299–302, 2009.
48. Nagre, S. S. and A. S. Shirsat, "Design of compact CPW-Fed printed monopole UWB antenna for band notched applications," *International Conference on Automatic Control and Dynamic Optimization Techniques (ICACDOT)*, 394–397, Pune, 2016.
49. Nguyen, T. D., D. H. Lee, and H. C. Park, "Design and analysis of compact printed triple band-notched UWB antenna," *IEEE Antennas and Wireless Propagation Letters*, Vol. 10, 403–406, 2011.
50. Nguyen, D. T., D. H. Lee, and H. C. Park, "Very compact printed triple band-notched UWB antenna with quarter-wavelength slots," *IEEE Antennas and Wireless Propagation Letters*, Vol. 11, 411–414, 2012.
51. Zaker, R., C. Ghobadi, and J. Nourinia, "Novel modified UWB planar monopole antenna with variable frequency band-notch function," *IEEE Antennas and Wireless Propagation Letters*, Vol. 7, 112–114, 2008.
52. Theepak, S. and S. Sinha, "UWB antenna designs with double band-notches for WLAN frequencies including time domain analysis," *Loughborough Antennas & Propagation Conference (LAPC)*, 1–5, Loughborough, 2012.
53. Vendik, I. B., A. Rusakov, K. Kanjanasit, J. Hong, and D. Filonov, "Ultrawideband (UWB) planar antenna with single-, dual-, and triple-band notched characteristic based on electric ring resonator," *IEEE Antennas and Wireless Propagation Letters*, Vol. 16, 1597–1600, 2017.
54. Rani, M. S. A., S. K. A. Rahim, M. R. Kamarudin, T. Peter, S. W. Cheung, and B. M. Saad, "Electromagnetic behaviors of thin film CPW-fed CSRR loaded on UWB transparent antenna," *IEEE Antennas and Wireless Propagation Letters*, Vol. 13, 1239–1242, Dec. 2014.
55. Emadian, S. R. and J. Ahmadi-Shokouh, "Very small dual band-notched rectangular slot antenna with enhanced impedance bandwidth," *IEEE Transactions on Antennas and Propagation*, Vol. 63, No. 10, 4529–4534, Oct. 2015.
56. Peng, L., B. Wen, X. Li, X. Jiang, and S. Li, "CPW fed UWB antenna by EBGs with wide rectangular notched-band," *IEEE Access*, Vol. 4, 9545–9552, 2016.